Energy Conservation Benefits of a Dedicated Outdoor Air System with Parallel Sensible Cooling by Ceiling Radiant Panels

Jae-Weon Jeong
Student Member ASHRAE

Stanley A. Mumma, Ph.D., P.E.
Fellow ASHRAE

William P. Bahnfleth, Ph.D, P.E.
Member ASHRAE

ABSTRACT

Dedicated outdoor air systems (DOAS) integrated with ceiling radiant cooling panels as a parallel sensible cooling system are being considered as an alternative to conventional variable air volume (VAV) systems for commercial buildings because of their energy conservation, first and operating costs, and indoor air quality advantages. A pilot DOAS/radiant panel cooling system is being constructed on a university campus to investigate its advantages over alternative cooling systems in a real application. Prior to the actual operation of the pilot system, the energy conservation potential of the DOAS/radiant cooling panel system relative to a VAV system with air-side economizer control was estimated. Hourly energy simulation predicts that the annual electrical energy consumption of the pilot DOAS/radiant panel cooling system is 42% less than that of the conventional VAV system with air-side economizer.

INTRODUCTION

All-air variable air volume (VAV) systems are widely used in many types of buildings, in spite of the fact that these common systems have several significant deficiencies. In order to meet the requirements of ASHRAE Standard 62-2001 (ASHRAE 2001), the multiple spaces method must be used to increase the outdoor air (OA) fraction at the air-handling unit. This increased outdoor air quantity may add significantly to energy consumption and operating cost but, unfortunately, does not guarantee that individual spaces will always, or ever, receive the intended outdoor air quantity (Mumma and Lee 1998). In addition, the part-load humidity problems associated with some VAV systems are well known.

The challenge of conforming to ASHRAE Standard 62-2001 in an energy efficient manner can be met with a dedicated outdoor air system (DOAS) in parallel with terminal sensible cooling equipment. A key concept of DOAS is the decoupling of sensible and latent loads. The DOAS provides 100% of the required ventilation air at constant volume and meets the full latent conditioning load (ventilation air latent load plus space latent load) and a portion of the space sensible load, while the terminal system meets only the remaining space sensible load (Mumma and Shank 2001). In addition, the DOAS does not use recirculated air. Any contaminants released inside the building are not transported to other parts of the building by the mechanical system, so building-wide contamination from a localized release will not occur (Mumma 2001a).

A properly designed DOAS with parallel sensible system can save considerable energy compared with a conventional system while always supplying the correct amount of ventilation air, as required by ASHRAE Standard 62-2001, to each space. There are many alternatives for the parallel sensible systems: conventional VAV systems, fan-coil units, and ceiling radiant panels. However, modeling and economic analysis indicate that ceiling radiant cooling panels are the best choice (Shank and Mumma 2001).

To test this conclusion empirically, a pilot DOAS/radiant panel cooling system is being installed in a studio at the Pennsylvania State University (Mumma 2001b). This paper presents modeling results comparing the energy consumption and other operating characteristics of the pilot system's performance with that of a VAV system serving the same space. The model of the pilot system has been developed using general purpose equation-solving software because existing energy simulation programs cannot model DOAS/radiant panel cooling system properly.

Jae-Weon Jeong is a doctoral student, **Stanley A. Mumma** is a professor, and **William P. Bahnfleth** is an associate professor in the Department of Architectural Engineering, the Pennsylvania State University, University Park, Penn.

OVERVIEW OF DECOUPLED SYSTEMS

Most of the problems in all-air VAV systems are caused by the fact that a single HVAC system is requested to perform too many tasks simultaneously. As a consequence of new findings in thermal comfort and indoor air quality (IAQ) requirements, new functions were superimposed mostly on the sensible heat transfer function of air in an air-handling system. Many researchers found serious problems in this "overloaded system" during the last decade and at last began to propose "decoupling" concepts; decoupling of ventilation and the air-conditioning function (Scofield and Des Champs 1993; Khattar and Brandemuehl 2002; Mumma and Lee 1998; Coad 1999) or decoupling of sensible and latent load functions (Kilkis et al. 1995; Mumma 2001d; Niu et al. 2002). Once these functions are decoupled, it becomes possible to employ a more dedicated and function-specialized system for each purpose.

System configurations that successfully decouple the sensible and latent functions of an HVAC system have been reported in the literature. Khattar and Brandemuehl (2002) investigated the performance of a dual-path system integrated with CO_2 demand-based ventilation control in which ventilation air and recirculation air were conditioned separately but delivered to the space through a common supply duct. Their results showed that the dual-path system provided 14% to 27% annual energy savings and 15% to 23% smaller equipment tonnage compared with a conventional VAV system.

Ceiling radiant cooling panel (CRCP) systems have been investigated in European countries (Wilkins and Kosonen 1992). That work illustrated the energy and thermal comfort benefits of the CRCP system combined with various ventilation systems. The ventilation systems investigated can be categorized into a mixing or displacement ventilation system (Brunk 1993; Behne 1995; Niu et al. 1995; Simmonds 1994, 1996). The three main advantages of CRCP systems deduced from the literature are: (1) large amounts of fan energy saving, (2) improved thermal comfort, and (3) simple and effective zone control. In practice, two different ventilation strategies, mixing and displacement ventilation, are usually combined with a CRCP system. A conventional all-air VAV system or a 100% OA conditioning system can be used for both ventilation strategies.

Külpmann (1993) and Niu and Kooi (1994) discussed the advantages of displacement ventilation on thermal comfort and indoor air quality (IAQ) compared with mixing ventilation systems. Busweiler (1993) proposed a 100% OA system for displacement ventilation, to be cooled and dehumidified by cooling coils or desiccant cooling systems to prevent condensation on the CRCP surface. Researchers have since used experimental and numerical methods to investigate displacement ventilation when combined with CRCP systems (Behne 1995; Tan et al. 1998; Hodder et al. 1998; Imanari et al. 1999).

Recently, Niu et al. (2002) proposed a 100% OA displacement ventilation system consisting of a desiccant cooling system combined with a chilled ceiling. In their concept, the sensible load is primarily treated by CRCPs, and the latent and ventilation loads are met by an auxiliary desiccant cooling system. They indicated that, theoretically, the CRCP system combined with desiccant cooling could save up to 44% of primary energy consumption in comparison with a conventional constant air volume (CAV) system.

On the other hand, Mumma (2002e) and Badenhorst (2002) indicated three reasons to employ mixing ventilation rather than displacement ventilation. First, the air movement across the chilled ceiling surface typically boosts the cooling performance by at least 5%. Second, the benefit of enhanced air quality that is typically realized by a displacement system cannot be achieved when combined with a CRCP system. The cooled ceiling convection currents cause the room air to become mixed, disturbing the otherwise stratified air, and contaminants will be mixed into rather than displaced out of the breathing zone. Third, large supply-to-room temperature differentials can be used with mixed flow systems, especially if high induction ratio diffusers are used, shifting more of the sensible cooling load to the DOAS and greatly reducing the first cost of the radiant cooling system.
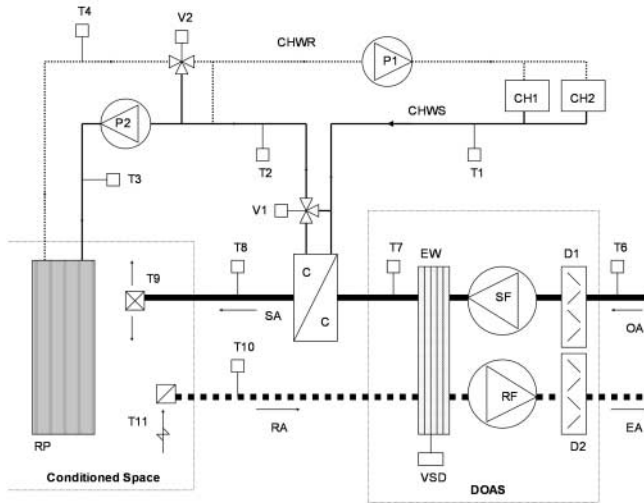
In addition, Sodec (1999) compared the annual energy consumption of two different ventilation strategies: mixing and displacement ventilation with a CRCP system. He showed that the displacement ventilation combined with a radiant panel system consumes 17% more energy compared with mixing ventilation with radiant panels. It comes from the fact that displacement ventilation requires higher SA temperature than mixed ventilation, and the cooled and dehumidified SA must be reheated before it is delivered to the space at floor level.

As one of several workable systems using the mixed ventilation strategy, Mumma (2001d) proposed the DOAS with CRCP system. In this system, conditioned 100% OA is supplied to a space through high induction diffusers; therefore, effective dehumidification can be achieved with minimal or no need for reheat. The energy, initial and operating costs, IAQ, and thermal comfort benefits of the DOAS with CRCP system, as well as control and condensation issues, have been addressed (Mumma 2001a, 2001c, 2001e, 2002a; Shank and Mumma 2001; Mumma 2001f, 2001g, 2002b).

PILOT DOAS/RADIANT PANEL COOLING SYSTEM

The 297.3 m² (3200 ft²) space to be cooled by the pilot DOAS/radiant panel cooling system has one single-glazed exterior exposure and three interior partitions adjacent to unconditioned spaces. The floor and ceiling are also adjacent to unconditioned spaces. The ceiling height is 4.3 m (14 ft), with pendent illumination at the 2.7-m (9-ft) plane. Design occupancy is 40 students.

The pilot system is shown schematically in Figure 1. Two 5-ton reciprocating air-cooled chillers connected in parallel cool 30% ethylene glycol/water solution flowing at the rate of 1.4 L/s (22 gpm). The system is composed of two chilled water loops: one serving the DOAS cooling coil (cooling coil loop)

Figure 1 *Pilot DOAS/radiant panel cooling system.*

and the other serving eight rows of radiant panels (panel loop). Each row has three 0.61 m × 3.96 m (2 ft × 13 ft) panels, and the eight rows are connected in parallel. The DOAS is a constant air volume, variable temperature system.

Two three-way control valves have been used to modulate glycol flow, one in the cooling coil circuit (V1) and the other in the radiant panel loop control valve (V2). Valve V1 is used to control the DOAS supply air temperature. The coil bypass chilled glycol mixes with the coil outlet glycol before becoming available to the radiant panel loop. Valve V2 is used to modulate the panel supply water temperature by mixing panel return glycol with the glycol from the cooling coil.

Control Sequence

Space cooling is achieved by a two-stage process. At low loads, the first stage of cooling is provided by a variable supply air temperature DOAS. As the cooling load increases, the DOAS supply air temperature drops to a low limit (11.1°C [52°F] in this case) that is sufficiently dry to maintain the space design dew-point temperature. If the space temperature remains higher than the thermostat setpoint (23.9°C [75°F]) when the DOAS is at full capacity, the second-stage radiant panel sensible cooling system is enabled. The radiant panels are not enabled until the space dew-point temperature (DPT) has been brought under control by the low supply air temperature. The temperature of the panel supply water is modulated to meet the balance of the space sensible load, constrained to be no colder than 0.56°C ~1.67°C (1°F ~3°F) higher than the space DPT, to prevent condensation on the panel surfaces. This control concept is carried out through the following sequence of operation:

1. Low ambient temperature cut out

    • If the OA temperature T6 (Figure 1) drops below –6.67°C (20°F) no part of the system is to oper-

ate since the DOAS will not have a preheat coil

2. DOAS fans, dampers

    • Supply and return fans operate during occupied mode
    • Enthalpy wheel drive enabled during the occupied mode

3. Space cooling temperature control

    • Modulate V1 to satisfy space temperature T9. Do not permit T8 to drop below a predetermined setpoint (11.1°C [52°F]).
    • If T8 is at low limit (11.1°C [52°F]) and T9 is above the space minimum setpoint (23.9°C [75°F]), activate pump P2 and modulate V2 as required to meet the space temperature setpoint with the radiant panels. T2 low limit is space DPT+1.67°C (3°F) to prevent condensate on the panel surface.
    • If the condensate sensor indicates water present, de-energize P2 and close V2.

4. Chiller Control

    • If OA temperature T6 is greater than –6.67°C (20°F) and the system is in occupied mode, pump P1 and CH1 are enabled. Return CHW bypasses inactivated CH2 and mixes with CHW coming from CH1, which supplies CHW at a temperature 6.67°C (44°F). The cooling coil receives CHW at the mixed temperature. If the cooling coil requires more than 1.4 L/s (22 gpm) of CHW, CH2 is enabled and supplies 6.67°C (44°F) CHW.

5. Enthalpy Wheel Control

    • If OA enthalpy > return air (RA) enthalpy, run enthalpy wheel at full speed (20 rpm)
    • If OA enthalpy ≤ RA enthalpy, and OA DPT > 11.1°C (52°F), enthalpy wheel is to be off.
    • If OA DPT ≤ 11.1°C (52°F), modulate the enthalpy wheel speed using variable-speed drive (VSD) to achieve an 11.1°C (52°F) DPT.

SYSTEM MODELING FOR ENERGY SIMULATION

Hourly space sensible and latent cooling loads determined with commercial software were used in the simulation. Given the hourly space sensible and latent cooling loads and the coincident OA loads based on hourly weather data and enthalpy wheel performance, the chilled water flow rates and inlet and outlet temperatures of the cooling coil and radiant panels were determined by applying mass and energy balances. The radiant cooling panel removed that portion of the space sensible not met with the DOAS supply air.

The three-way valve operation can also be modeled with mass and energy balances. The cooling load on the radiant panels, when operating, is the difference between the space sensible load and the space cooling done by the DOAS supply air.

TABLE 1
Coefficients for Reciprocating Air-Cooled Electrical Chiller Model

Curves	a	b	c	d	e	f
CAP_FT	0.57617295	0.02063133	0.00007769	-0.00351183	0.00000312	-0.00007865
EIR_FT	0.66534403	-0.01383821	0.00014736	0.00712808	0.00004571	-0.00010326
EIR_FPLR	0.11443742	0.54593340	0.34229861			

The supply and return fans and two pumps in this system are constant volume devices; therefore, their energy consumption can be calculated easily. On the other hand, the reciprocating chiller and enthalpy wheel must be modeled in more detail to give a sufficiently accurate representation of their off-design performance as cooling loads and ambient conditions change.

Reciprocating Air-Cooled Chiller Model

A generic reciprocating air-cooled chiller model (California Energy Commission 2001) was used in the system simulation. This model returns the power consumption of the chiller in kW given the rated capacity, rated full-load power, cooling load, OA dry-bulb temperature, and chilled water supply temperature.

$$Q_{available}(T_{chws}, T_{odb}) = \text{CAP\_FT} \times Q_{rated} \qquad (1)$$

$$\text{CAP\_FT} = a + b \cdot (1.8 \times T_{chws} + 32) + c \cdot (1.8 \times T_{chws} + 32)^2$$
$$+ d \cdot (1.8 \times T_{odb} + 32) + e \cdot (1.8 \times T_{odb} + 32)^2 \qquad (2)$$
$$+ f \cdot (1.8 \times T_{chws} + 32) \cdot (1.8 \times T_{odb} + 32)$$

where,

$Q_{available}$ = available cooling capacity at present evaporator and condenser conditions (kW)

CAP_FT = cooling capacity adjustment curve (Table 1)

Q_{rated} = cooling capacity at rated conditions (kW)

T_{chws} = chilled water supply temperature (°C)

T_{odb} = outside-air dry-bulb temperature (°C).

$$P_{operating} = P_{rated} \times \text{EIR\_FPLR} \times \text{EIR\_FT} \times \text{CAP\_FT} \qquad (3)$$

$$\text{EIR\_FPLR} = a + b \cdot PLR + c \cdot PLR^2 \qquad (4)$$

$$PLR = \frac{Q_{operating}}{Q_{available}} \qquad (5)$$

$$\text{EIR\_FT} = a + b \cdot (1.8 \times T_{chws} + 32) + c \cdot (1.8 \times T_{chws} + 32)^2$$
$$+ d \cdot (1.8 \times T_{odb} + 32) + e \cdot (1.8 \times T_{odb} + 32)^2 \qquad (6)$$
$$+ f \cdot (1.8 \times T_{chws} + 32) \cdot (1.8 \times T_{odb} + 32)$$

where

$P_{operating}$ = power consumption at the present operating condition (kW)

P_{rated} = rated power consumption (kW)

$Q_{operating}$ = operating cooling capacity at present evaporator and condenser conditions (kW)

EIR_FPLR = cooling efficiency adjustment curve, a function of part-load ratio (Table 1)

PLR = part-load ratio

EIR_FT = cooling efficiency adjustment curve (Table 1)

Enthalpy Wheel Model for DOAS

An enthalpy wheel recovers both sensible and latent energy in the DOAS. Its effectiveness is changed by modulating the rotational speed of the wheel. The enthalpy wheel operates in three modes: full speed, off, and modulated speed to achieve the supply air DPT setpoint. The operating mode is determined by the relationship between the OA enthalpy and RA enthalpy or OA DPT and supply air (SA) DPT setpoint (Mumma and Shank 2001).

Full speed operation: When the OA enthalpy (h_{oa}) is higher than the RA enthalpy (h_{ra}), the enthalpy wheel rotates at full speed for maximum sensible and latent effectiveness (80% in this case).

Wheel off operation: When h_{oa} is lower than h_{ra} and the OA DPT is higher than the SA DPT setpoint (11.1°C [52°F] in this case), the enthalpy wheel should be off. If the wheel operates in this condition, the enthalpy of SA after the enthalpy wheel increases, and the cooling coil load increases.

Speed modulation: When OA DPT is lower than SA DPT setpoint, the enthalpy wheel speed will be modulated by VSD to maintain this setpoint.

To develop a simulation model of an enthalpy wheel, functions related to wheel performance were derived from manufacturer's empirical data that show the variation of latent and sensible effectiveness according to the change of wheel rotating speed and driving force ratio (DFR, defined by Equation 7). DFR represents the ratio of latent energy (Q_{lat}) to sensible energy (Q_{sen}) transferred by an enthalpy wheel divided by the square of fractional OA relative humidity (RH). For the enthalpy wheel used in this model, the sensible effectiveness (SE) leads the latent effectiveness (LE) when the DFR is less than 1.5, and for DFR greater than 1.5, the LE leads the SE; for example, when RA is 22.2°C (72°F) DBT/50% RH and OA is 5.6°C (42°F) DBT/ 90% RH, humidity ratios of RA and OA are 0.0083 kg/kg

TABLE 2
Coefficients for Enthalpy Wheel Speed Function

LE	C1	C2	C3	C4	C5	C6
< 50%	2.344	−3.714	1.444	−0.005421	0.002286	0.05852
≥ 50%	−21.28	4.652	28.5	0.6905	−0.00218	−0.4167

LE	C7	C8	C9
< 50%	−0.0431	−0.001676	0.0006397
≥ 50%	−0.8788	0.004481	0.006532

(58 grain/lbm) and 0.0053 kg/kg (37 grain/lbm), respectively. For these conditions, from Equation 7, DFR is 0.54, so the SE leads the LE.

In design calculations, it is usually assumed that the SE and LE are equal for any wheel speed. This condition is true when the enthalpy wheel is at full speed, but not under other operating modes. Whenever the enthalpy wheel isn't operated at full speed, the SE leads the LE, or the LE leads the SE depending upon the value of the DFR and wheel manufacturer. When the enthalpy wheel rotates at full speed (20 rpm) the LE is at its maximum value (80%). If the wheel speed should be modulated to maintain SA DPT setpoint, Equation 8 can be used to determine required LE.

$$DFR = \frac{Q_{lat}}{Q_{sen}} \times \frac{1}{(RH_{oa}/100)^2}$$

$$= 2430.6 \times \frac{(HR_{ra} - HR_{oa})/(DBT_{ra} - DBT_{oa})}{(RH_{oa}/100)^2}$$

$$(7)$$

$$LE = 80\%, \qquad \text{at full-speed operation mode} \qquad (8a)$$

$$LE = \frac{HR_{sa.set} - HR_{oa}}{HR_{ra} - HR_{oa}} \times 100, \qquad \text{at speed modulation mode}$$

$$(8b)$$

where

DFR = driving force ratio

LE = latent effectiveness (%)

HR_{ra} = return air humidity ratio (kg/kg)

HR_{oa} = outdoor air humidity ratio (kg/kg)

$HR_{sa.set}$= supply air humidity ratio at 11.1°C (52°F) SA DBT setpoint

HR_{sa} = supply air humidity ratio after the enthalpy wheel (kg/kg)

RH_{oa} = outdoor air relative humidity (%)

DBT_{ra} = return air dry-bulb temperature (°C)

DBT_{oa} = outdoor air dry-bulb temperature (°C)

DBT_{sa} = supply air dry-bulb temperature after enthalpy wheel (°C)

Once DFR and LE are known, the enthalpy wheel speed and SE can be determined from the Equations 9 and 10. The wheel speed is a function of LE and DFR. For more accurate results, coefficients were calculated for two different latent effectiveness ranges: 0% < LE < 50% and 50% ≤ LE < 80%. The SE is a function of wheel speed. If SE and LE are known for any wheel rotating speed, the supply air humidity ratio and DBT leaving the enthalpy wheel can be obtained from Equations 11 and 12, respectively.

$$Spd = c_1 + c_2(DFR) + c_3(DFR)^2 + c_4(LE) + c_5(LE)^2$$
$$+ c_6(DFT)(LE) + c_7(DFR)^2(LE) \qquad (9)$$
$$+ c_8(DFR)(LE)^2 + c_9(DFR)^2(LE)^2$$

$$SE = 13.844 \cdot ln(Spd) + 38.469 \qquad (10)$$

$$HR_{sa} = (LE/100) \cdot (HR_{ra} - HR_{oa}) + HR_{oa} \qquad (11)$$

$$DBT_{sa} = (SE/100) \cdot (DBT_{ra} - DBT_{oa}) + DBT_{oa} \qquad (12)$$

where

SE = sensible effectiveness (%)

Spd = enthalpy wheel speed (rpm) (Table 2)

Enthalpy Wheel Simulation

To verify how well the enthalpy wheel model reproduces the manufacturer's data, the enthalpy wheel rotating speed was calculated for various LE and DFR values using Equation 9 and compared with actual speed data. Table 3 shows that the calculated speeds are very close to the manufacturer's data. Equation 10, the SE equation, was also developed from the manufacturer's SE versus speed data. The R^2 value, or the coefficient of determination, of Equation 10 is 0.9896.

Figure 2 shows the enthalpy wheel control characteristic. When the OA enthalpy (h_{oa}) is higher than RA enthalpy (h_{ra}), the enthalpy wheel rotates at full speed (Figure 2a), giving the maximum sensible and latent effectiveness of 80%. On the other hand, when the OA enthalpy (h_{oa}) is lower than RA enthalpy (h_{ra}) (Figure 2a) and the OA DPT is higher than the SA DPT (Figure 2b), the enthalpy wheel is turned off. Finally, when the OA DPT is lower than the SA DPT, the enthalpy wheel speed is modulated to maintain SA DPT of 11.1°C (52°F) (Figure 2b).
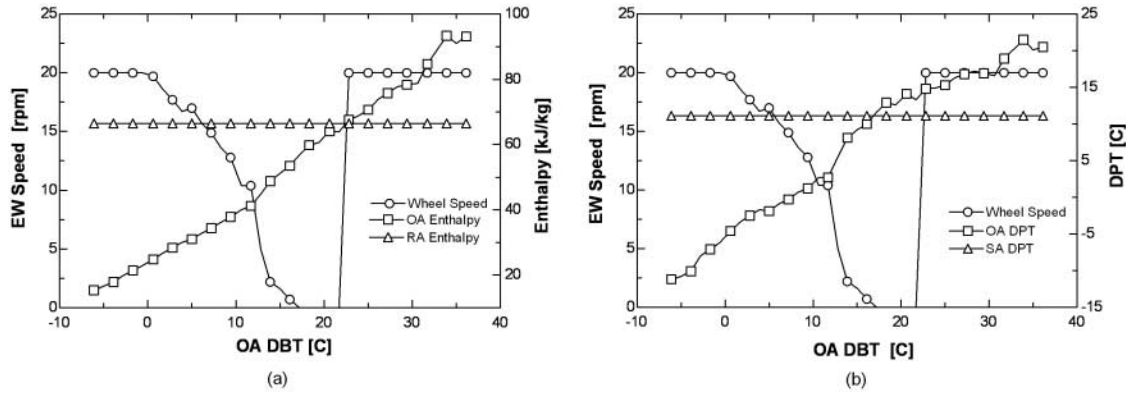
Figure 2 *(a) OA and RA enthalpy effect, (b) OA and SA DPT effect on wheel speed control.*

TABLE 3
Calculated Rotating Speed (rpm) vs. Actual Speed Data

LE [%]	5		10		20		30		40		50		60		70		80	
DFR	M*	C**	M	C	M	C	M	C	M	C	M	C	M	C	M	C	M	C
0.1	2	2	2.2	2.2	2.9	2.8	3.9	3.9	5.1	5.4	7.3	7.3	11.6	11.9	16.1	16.1	20	20
0.4	1.2	1.2	1.4	1.4	2.0	2.0	2.9	3.0	4.0	4.3	5.9	5.9	10.2	10.5	15.3	15.2	20	20
0.75	0.3	0.5	0.7	0.7	1.3	1.2	2.1	2.0	3.1	3.2	4.6	4.6	8.2	8.7	14.2	13.9	20	20
1.0	0.2	0.2	0.3	0.3	0.8	0.8	1.5	1.5	2.3	2.5	3.7	3.7	6.0	7.4	12.8	12.8	20	20
1.25	0.1	0.1	0.2	0.1	0.4	0.4	1.0	1.0	1.6	1.9	2.7	3.0	4.7	5.9	11.3	11.6	20	20
1.75	0.1	0.1	0.1	0.1	0.2	0.1	0.4	0.4	1.0	1.0	1.8	1.8	3.3	2.7	8.8	8.8	20	20

* Manufacture's data
** Calculated speed using Equation (9)

Sensible Cooling Loads for DOAS and Radiant Panels

A DOAS system, by design, can always meet the entire space latent load. However, it will generally meet only a part of the peak space sensible load. If the space sensible load exceeds the DOAS sensible cooling capacity, this excess sensible load is met by the panel. The peak design sensible cooling load for the pilot system is 21.37 kW (72,900 Btu/h), and the maximum sensible cooling capacity of DOAS in the pilot system is 8.73 kW (29,800 Btu/h). Consequently, the maximum cooling capacity of the radiant panels in the pilot system is 12.64 kW (43,100 Btu/h). Therefore, when the space sensible load is higher than DOAS cooling capacity, radiant panel cooling is activated to remove the remaining sensible load (Figure 3). When the space sensible load is lower than the DOAS maximum sensible cooling capacity, the radiant panel is turned off and the DOAS SA temperature is modulated to match the space load (Figure 3).

Chiller Simulation

Figure 4 shows the supply and return CHW temperature variations. When the cooling load is sufficiently high, both chillers operate simultaneously and supply 6.67°C (44°F) CHW. When the cooling load is low, CH2 is off and bypassed and CHW supply temperature increases above 6.67°C (44°F). When chiller load decreases, CHW temperature difference between supply and return also becomes smaller. In the pilot DOAS/radiant panel system, the hot gas bypass method is used for chiller cooling capacity control. Hot gas bypass works by diverting hot gas from the compressor discharge into the evaporator and allows the machine to run even under a zero load condition. This method gives good capacity control but wastes energy at low loads.

ENERGY CONSERVATION IN DOAS/RADIANT PANEL COOLING SYSTEM

To compare the energy consumption of the pilot system with that of a conventional VAV system, two hourly annual energy simulations were done. The VAV system was simulated using a commercial whole-building energy simulation program and the DOAS/radiant panel cooling pilot system was modeled by the custom simulation described above. It was
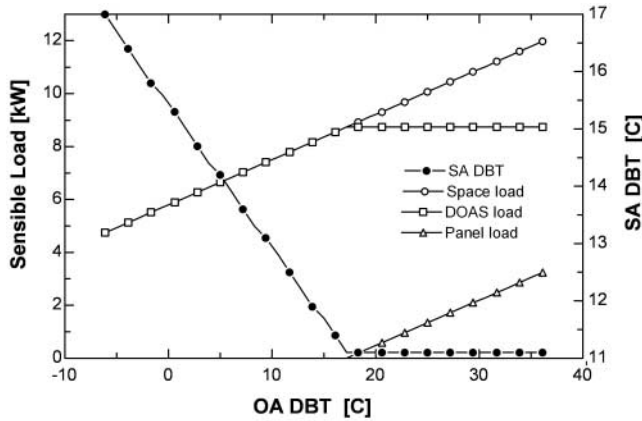
Figure 3 *Sensible loads and SA temperature reset.*

Figure 4 *CHW supply and return temperature.*

assumed that the VAV had integrated air-side economizer and demand-based ventilation control.

The same calculated hourly space cooling loads were used as input data in both simulations. It was assumed that both systems operate from 8 a.m. to 7 p.m., that occupancy was constant at 40 people during those hours, and that infiltration effects were negligible. The same TMY weather data were also used in both simulations. The generic equipment models for a reciprocating air-cooled chiller, pump, and fan were used to estimate the energy consumption of each system. Consequently, the energy consumption for each system was estimated on a common base.

The DOAS/radiant panel cooling system follows the control scheme described above. The latent cooling load is always met by the DOAS. When the sensible cooling load exceeds the full capacity of the DOAS, the radiant panels are activated to meet remaining space sensible cooling load. Figure 5 clearly shows this characteristic of the DOAS/radiant panel cooling system. When the total space cooling load exceeds the DOAS cooling capacity, the radiant panel system accommodates the remaining cooling load.

Cooling Coil Load Reduction

In conventional all-air VAV systems, all the space cooling loads and OA ventilation cooling load are met by the cooling coils in the air-handling units. On the other hand, in the DOAS/radiant panel cooling system, the entire latent load, a portion of sensible load, and OA ventilation cooling load are handled by a combination of the enthalpy wheel and the DOAS cooling coil working in series. The radiant panel system accommodates the remaining sensible load. Therefore, the equivalent cooling coil load on the DOAS/radiant panel cooling system is the sum of DOAS cooling coil and the radiant panel loads.

In Figure 6, the equivalent cooling coil load annual duration curve of the pilot system is compared with that of the VAV system. The peak cooling coil loads of the VAV and the pilot system are 64.1 kW (218.8 kBtu/h) and 27.8 kW (94.8 kBtu/h), respectively. Thus, 57% of the peak cooling coil load was reduced by the enthalpy wheel in the DOAS/radiant panel cooling system.
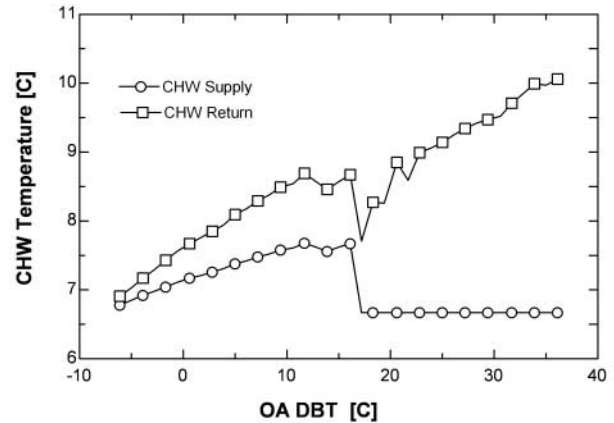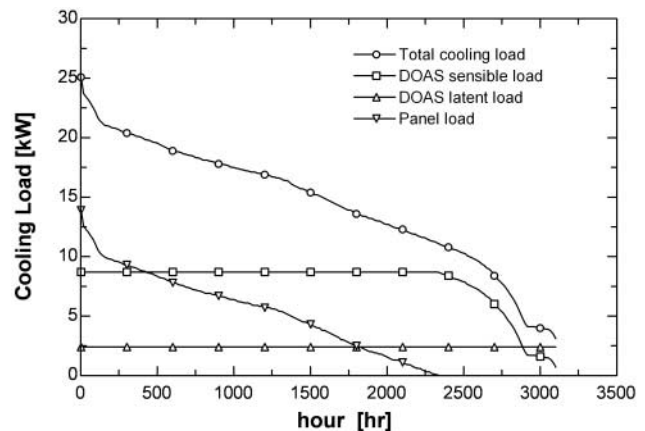

Figure 5 *Duration curves for DOAS and radiant panel cooling loads.*
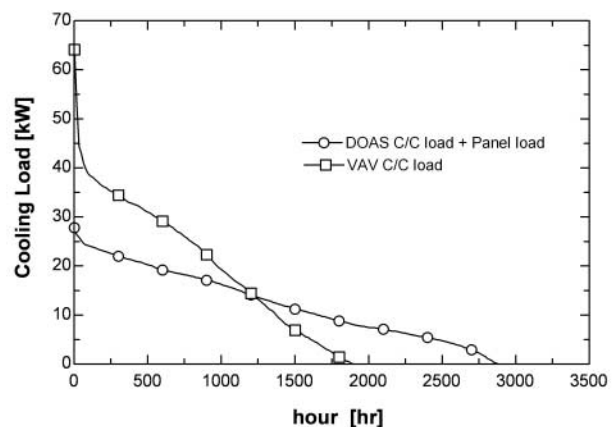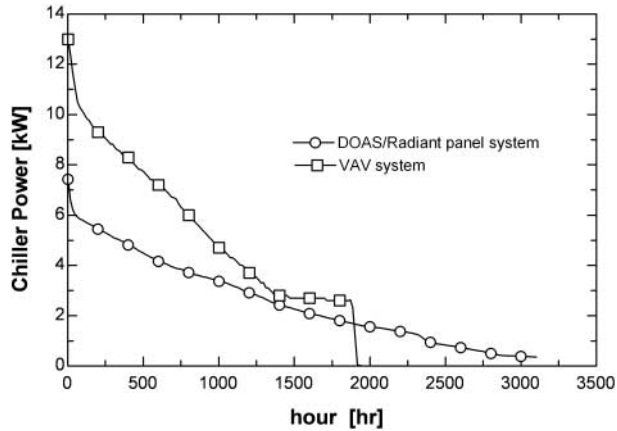

Figure 6 *Cooling coil load duration curves.*

In the pilot system, a design SA temperature of 11.1°C (52°F) was used with more ventilation air than required by ASHRAE Standard 62-2001. Total energy recovery was not analyzed in the VAV case since it is rarely used in practice for economic reasons (Mumma 2002a).

Figure 7 *Chiller energy consumption duration curves.*

Figure 8 *Pumping energy consumption duration curves.*

Because of air-side economizer operation, the total chiller operating hours of the VAV system are fewer than those of the pilot system. The chiller in the VAV system operated 1885 hours during the simulated year while the chiller in the pilot system operated for 3102 hours. However, the chiller cooling for the VAV system was 39 MWh/y (133 MBtu/y) while the chiller cooling of the pilot system was 36 MWh/yr (123 MBtu/y), so the chiller cooling was 7.6% less for the DOAS/radiant cooling panel system.
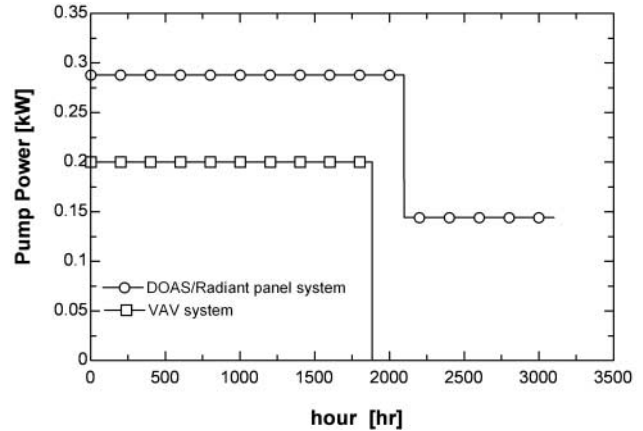
Chiller Energy Reduction

On the basis of the plant design load calculation, a 14 ton, 1.0 kW/ton air-cooled chiller was selected for the VAV case, and two 5 ton, 1.0 kW/ton air-cooled chillers were used for the pilot system, a 29% reduction in capacity requirement, because of the total energy recovery. The chiller part-load characteristics for both VAV and DOAS/radiant panel systems were identical.

Figure 7 shows the chiller energy consumption duration curves for both cases. Since the cooling coil operating hours have been reduced by the air-side economizer control in the VAV system, the chiller operating hours are smaller than those of the DOAS/radiant panel cooling system. The chillers for the VAV system and DOAS/radiant panel cooling system ran for 1885 hours and 3102 hours, respectively, during the simulated year. The DOAS/radiant panel cooling system chillers, however, consumed less energy for a year compared with the VAV system. The chiller for the VAV case consumed 10.6 MWh/y (seasonal COP of 3.7) while the chillers for the pilot system consumed 7.9 MWh/y (seasonal COP of 4.5), an annual chiller energy savings of 25% for the pilot system.

Pumping Energy Consumption

The DOAS/radiant panel cooling system consumes more pumping energy than the VAV system because it must circulate chilled water through the radiant panel loop as well as the DOAS cooling coil. Figure 8 clearly shows that the DOAS/radiant panel cooling system pumps are operated for more

hours during a year and always require more power than the VAV case. The yearly total pumping energy consumptions for the VAV and the pilot system are 0.38 MWh/y and 0.75 MWh/y, respectively. The pilot system consumes nearly twice as much pumping energy, 0.37 MWh/y. However, this penalty is counterbalanced by the greatly decreased fan energy and chiller energy consumptions of the DOAS system.

Fan Energy Reduction

The DOAS is a constant volume, variable temperature system, and the electric power required to operate the supply and return fans is constant when the system is on. The DOAS can provide exactly the minimum amount of ventilation air required by ASHRAE Standard 62-2001 as the supply air quantity. In the pilot system, the required SA flow rate could be as little as 376 L/s (40 people × 9.4 L/s/person) (800 scfm [40 people × 20 scfm/person]); however, 566 L/s (1200 scfm) was used as SA flow rate for safety.

On the other hand, the VAV system is a variable volume, constant temperature system, and the fan power changes with the varying air volume. The VAV system always consumes much more fan energy than the DOAS because of its much higher SA and RA flow rates. The design SA flow rate for the VAV system simulation was 1520 L/s (3220 scfm), 2.7 times higher than DOAS design SA flow rate. In other words, the DOAS design SA quantity is only 37% of the design VAV flow rate.

Figure 9 clearly shows that the fans used in the VAV system always require more power than the DOAS fans. The yearly total fan energy consumption for the VAV system and DOAS was 7.97 MWh/y and 2.33 MWh/y, respectively. DOAS fan energy consumption is only 29% of the VAV case for a year.

Total Energy Consumption Comparison

In the preceding sections, the chiller, pump, and fan energy consumptions for both systems have been compared separately. The total energy consumption characteristic is the
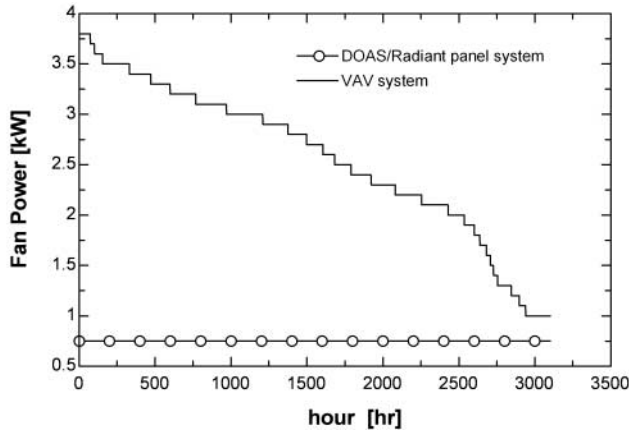
Figure 9   *Fan energy consumption duration curves.*

Figure 10   *Total energy consumption duration curves.*

sum of these three energy consumption components for each system. Comparison of these aggregate numbers clearly shows the superiority of the DOAS/radiant panel cooling system.

An annual total energy duration curve (Figure 10) shows that the DOAS/radiant panel cooling system consumes less energy during most of the year and is at worst comparable in energy consumption during low-load hours. In terms of the peak power demand, the VAV system requires 17 kW at its peak time while the DOAS/radiant panel cooling system has a peak demand of only 8.5 kW, which is 50% of the VAV system peak.

The yearly total energy consumption for each system with breakdown by components is shown in Figure 11. The chiller and the fan energy consumption of the pilot system is smaller than those of the VAV case except the pumping energy consumption.

Note that the fan energy has been reduced dramatically by the new system. Finally, the total energy consumption for the VAV system and the pilot system is 18.92 MWh/y and 10.98 MWh/y, respectively, so the DOAS/radiant panel cooling system saved 42% annually compared with the conventional all-air VAV system with air-side economizer control.

CONCLUSIONS

Energy simulation results comparing the pilot DOAS/radiant panel cooling system with a conventional all-air VAV system with air-side economizer are as follows:

- The chiller energy consumption of the pilot system is 25% less than the VAV case. From the design load calculation, the chiller size is already reduced by 29% because of the total energy recovery and small SA quantity of DOAS.
- The DOAS cooling coil load plus radiant panel cooling load is reduced by 7.6% annually compared with VAV system cooling coil.
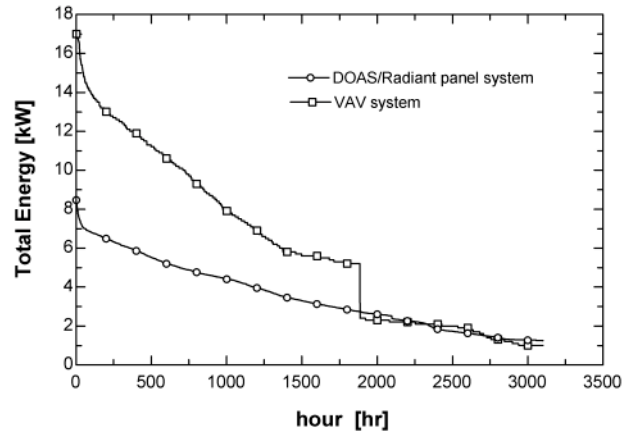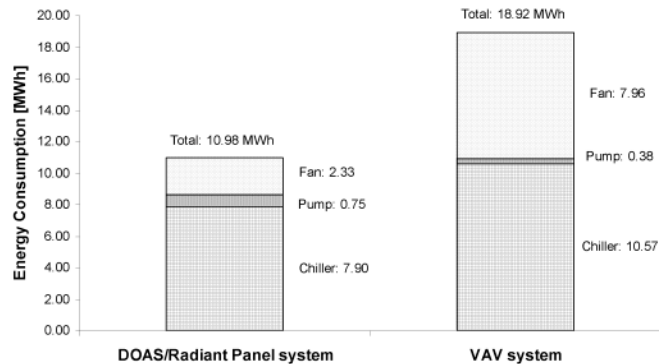- The pilot system needs nearly twice as much pumping

Figure 11   *Yearly total energy consumption comparison.*

energy compared with VAV case.

- DOAS fans consume energy only 29% of the VAV case because of very small SA and RA quantity.
- Finally, the pilot DOAS/radiant panel cooling system can save 42% of total energy consumption annually compared with the case of a conventional all-air VAV system with economizer control.

Although the above simulation results are specific to the pilot system, it is enough to show the possibility of energy conservation achieved by the DOAS/radiant panel cooling system. In general, the DOAS/radiant panel cooling system consumes more pumping energy compared with the conventional all-air VAV system because more pumps are required to circulate CHW through radiant panels. However, this increased pumping energy is more than offset by the greatly decreased fan and chiller energy, which mainly comes from the total energy recovery.

REFERENCES

ASHRAE. 2001. *ASHRAE Standard 62-2001, Ventilation for acceptable indoor air quality.* Atlanta: American Soci-

ety of Heating, Refrigerating and Air-Conditioning Engineers, Inc.

Badenhorst. 2002. Chilled ceilings and chilled beams. *IRHACE Technical Conference 2002*. Christchurch, New Zealand: Institute of Refrigeration, Heating and Air-Conditioning Engineers.

Behne, M. 1995. Is there a risk of draft in rooms with cooled ceilings? Measurement of air velocities and turbulences. *ASHRAE Transactions* 101(2): 744-752.

Brunk, M.F. 1993. Cooling ceilings—An opportunity to reduce energy costs by way of radiant cooling. *ASHRAE Transactions* 99(2): 479-487.

Busweiler, U. 1993. Air conditioning with a combination of radiant cooling, displacement ventilation, and desiccant cooling. *ASHRAE Transactions* 99(2): 503-510.

California Energy Commission. 2001. *AB970 Nonresidential Alternative Calculation Method Approval Manual*. Energy Commission Publication No. P 400-01-003.

Coad, W.J. 1999. Conditioning ventilation air for improved performance and air quality. *Heating/Piping/Air-conditioning* Sept.: 49-56.

Hodder, S.G., D.L. Loveday, K.C. Parsons, and A.H. Taki. 1998. Thermal comfort in chilled ceiling and displacement ventilation environments: vertical radiant temperature asymmetry effects. *Energy and Buildings* 27: 167-173.

Imanari, T., T. Omori, and K. Bogaki. 1999. Thermal comfort and energy consumption of the radiant ceiling panel system. Comparison with the conventional all-air system. *Energy and Buildings* 30: 167-175.

Khattar, M.K., and M.J. Brandemuehl. 2002. Separating the V in HVAC: A dual-path approach. *ASHRAE Journal* May: 37-42.

Kilkis, B.I., S.R. Suntur, and M. Sapci. 1995. Hybrid HVAC systems. *ASHRAE Journal* Dec.: 23-28.

Külpmann, R.W. 1993. Thermal comfort and air quality in rooms with cooled ceilings—results of scientific investigations. *ASHRAE Transactions* 99(2): 488-502.

Mumma, S.A., and B.W. Lee. 1998. Extension of the multiple spaces concept of ASHRAE Standard 62 to include infiltration, exhaust/exfiltration, interzonal transfer, and additional short circuit paths. *ASHRAE Transactions* 104(2): 1232-1241.

Mumma, S.A. and K.M. Shank. 2001. Achieving dry outside air in an energy-efficient manner. *ASHRAE Transactions* 107(1): 553-561.

Mumma, S.A. 2001a. Safety and Comfort using radiant cooling panel system. *IAQ Applications/Winter 2001*: 17-19.

Mumma, S.A. 2001b. Dedicated outdoor air in parallel with chilled ceiling system. *Engineered Systems*. Nov. 2001: 56-66.

Mumma, S.A. 2001c. Ceiling panel cooling system. *ASHRAE Journal* Nov. 2001: 28-32.

Mumma, S.A. 2001d. Overview of integrating dedicated outdoor air systems with parallel terminal systems. *ASHRAE Transactions* 107(1): 545-552.

Mumma, S.A. 2001e. Preconditioning dedicated OA for improved IAQ —Part 2. *IAQ Application/Summer 2001*: 21-23.

Mumma, S.A. 2001f. Dedicated outdoor air—Dual wheel system control requirements. *ASHRAE Transactions* 107(1): 147-155.

Mumma, S.A. 2001g. Condensation issues with radiant cooling panels. *IAQ Applications/Fall 2001*:16-18.

Mumma, S.A. 2002a. Economics of improved environmental quality. *IAQ Applications/Spring 2002*: 15-18.

Mumma, S.A. 2002b. Chilled ceilings in parallel with dedicated outdoor air systems: Addressing the concerns of condensation, capacity, and cost. *ASHRAE Transactions* 108(2): 220-231.

Niu, J.L., and J.V.D. Kooi. 1994. Thermal climate in rooms with cool ceiling systems. *Building and Environment* 29: 283-290.

Niu, J.L., J.v.d. Kooi, and H.v.d. Ree. 1995. Energy saving possibilities with cooled-ceiling systems. *Energy and Buildings* 23: 147-158.

Niu, J.L., L.Z. Zhang, and H.G. Zuo. 2002. Energy savings potential of chilled-ceiling combined with desiccant cooling in hot and humid climates. *Energy and Buildings* 34: 487-495.

Scofield, M., and N.H. Des Champs. 1993. HVAC design for classrooms: Divide and conquer. *Heating/Piping/Air-Conditioning* May: 53-59.

Shank, K.M., and S.A. Mumma. 2001. Selecting the supply air conditions for a dedicated outdoor air system working in parallel with distributed sensible cooling terminal equipment. *ASHRAE Transactions* 107(1): 562-571.

Simmonds, P. 1994. Control strategies for combined heating and cooling radiant systems. *ASHRAE Transactions* 100(1): 1031-1039.

Simmonds, P. 1996. Practical applications of radiant heating and cooling to maintain comfort conditions. *ASHRAE Transactions* 102(1): 659-666.

Sodec, F. 1999. Economic viability of cooling ceiling systems. *Energy and Buildings* 30: 195-201.

Tan, H., T. Murata, K. Aoki, and T. Kurabuchi. 1998. Cooled ceiling/Displacement ventilation hybrid air conditioning system—Design criteria. *Proceeding of Roomvent '98* (1): 77-84.

Wilkins, C.K. and R. Kosonen. 1992. Cool ceiling system: a European air-conditioning alternative. *ASHRAE Journal* Aug.: 41-45.